Probing the structures and chemical bonding of boron-boronyl clusters using photoelectron spectroscopy and computational chemistry: B4(BO) n − (n = 1–3)

Qiang Chen, Hua-Jin Zhai, Si-Dian Li, and Lai-Sheng Wang

Citation: The Journal of Chemical Physics **137**, 044307 (2012); doi: 10.1063/1.4737863
View online: http://dx.doi.org/10.1063/1.4737863
View Table of Contents: http://scitation.aip.org/content/aip/journal/jcp/137/4?ver=pdfcov
Published by the AIP Publishing

Probing the structures and chemical bonding of boron-boronyl clusters using photoelectron spectroscopy and computational chemistry: $B_4(BO)_n^-$ ($n = 1$–3)

Qiang Chen,[1] Hua-Jin Zhai,[1,2] Si-Dian Li,[1,a)] and Lai-Sheng Wang[2,b)]
[1]*Institute of Molecular Sciences, Shanxi University, Taiyuan 030006, China*
[2]*Department of Chemistry, Brown University, Providence, Rhode Island 02912, USA*

(Received 23 May 2012; accepted 5 July 2012; published online 27 July 2012)

The electronic and structural properties of a series of boron oxide clusters, B_5O^-, $B_6O_2^-$, and $B_7O_3^-$, are studied using photoelectron spectroscopy and density functional calculations. Vibrationally resolved photoelectron spectra are obtained, yielding electron affinities of 3.45, 3.54, and 4.94 eV for the corresponding neutrals, B_5O, B_6O_2, and B_7O_3, respectively. Structural optimizations show that these oxide clusters can be formulated as $B_4(BO)_n^-$ ($n = 1$–3), which involve boronyls coordinated to a planar rhombic B_4 cluster. Chemical bonding analyses indicate that the $B_4(BO)_n^-$ clusters are all aromatic species with two π electrons. © *2012 American Institute of Physics*. [http://dx.doi.org/10.1063/1.4737863]

I. INTRODUCTION

As an electron-deficient element, boron and its compounds exhibit intriguing chemical bonding properties.[1,2] Concepts, such as the three-center two-electron (3c-2e) bond in boranes, have played an essential role in advancing modern chemical bonding models.[3,4] In comparison to its neighbor in the periodic table, however, elemental boron clusters have received relatively less experimental attention.[5] Earlier computational studies show that the three-dimensional (3D) cage structures, common in bulk boron, are not stable for isolated boron clusters, which are more stable as planar (2D) or quasi-planar structures.[6,7] Joint photoelectron spectroscopy (PES) and computational studies over the past decade have revealed that size-selected boron clusters, B_n^-, are planar up to at least $n = 21$.[8–17] These clusters are shown to be aromatic or antiaromatic following the $(4N + 2)$ and $4N$ Hückel rules, and have been viewed as all-boron analogs of the hydrocarbons.[12,13] The 2D-to-3D transition was first suggested to occur at B_{20} for neutral clusters,[14] which has been corroborated by more recent computational studies,[18,19] and at B_{16}^+ for cationic clusters.[20] But the 2D-to-3D transition is not known for anionic B_n^- clusters yet. Electron delocalization and aromaticity are found to be key bonding features for the electron-deficient boranes and the planar boron clusters.[8–17,21] Recent computational studies suggest that infinitively large 2D boron layers are possible,[22] which feature hexagonal "holes" within a triangular lattice and also display delocalized bonding.[23]

Oxidation of boron is of interest in the combustion of boron and boranes, which is relevant to the development of energetic boron-based propellants.[24] The simplest boron oxide is the diatomic boronyl (BO) species, which is a σ-radical with a B≡O triple bond.[25,26] However, the structures and bonding in boron oxide clusters have remained largely unexplored.[27–32] Boron oxide clusters have been topics of some recent computational studies.[33–36] BO and BO^- are valent isoelectronic to CN and CN^-, respectively, which are important ligands in chemistry and biochemistry; analogous chemistry may exist for BO and BO^-. Recently, the first compound containing a boronyl has been synthesized in the bulk.[37]

We have been interested in understanding the electronic and structural properties of boron oxide clusters using PES and quantum chemical calculations.[26,38–43] We have shown that boron-rich oxide clusters can be formulated as boronyl ligands coordinated to boron clusters. For example, the $B_3O_2^-$, $B_4O_3^-$, and $B_5O_4^-$ clusters possess linear $B(BO)_2^-$ ($D_{\infty h}$, $^3\Sigma_g$), triangular $B(BO)_3^-$ (D_{3h}, $^2A_2''$), and tetrahedral $B(BO)_4^-$ (T_d, $^1A_1$) global minimum structures,[39,41] respectively, whereas the $B_4O_2^{2-}$ cluster adopts the linear diboronyl diborene $B_2(BO)_2^{2-}$ ($D_{\infty h}$, $^1\Sigma_g^+$) global minimum structure with a B≡B triple bond.[40] These clusters can be viewed as boronyl ligands coordinated to a B or B_2 core, analogous to boranes: BH_n^- ($n = 2$–4) and $B_2H_2^{2-}$, respectively.[39–41] In a more recent study, we discovered bridging η^2-BO groups in $B_2(BO)_3^-$ (C_{2v}, $^1A_1$) and $B_3(BO)_3^-$ (C_s, $^2A'$) clusters,[43] which are analogous to the 3c-2e BHB bond in $B_2H_3^-$ and $B_3H_3^-$. Thus, the boronyl group can act as either a terminal or bridging ligand and is capable of forming 3c-2e bridging bonds, showing isolobal analogy between boron-rich oxide clusters and boranes.

In the current article, we report an investigation on the structures and bonding of a new series of boron oxide clusters: B_5O^-, $B_6O_2^-$, and $B_7O_3^-$ using PES and computational chemistry. Vibrationally resolved PES spectra are obtained for all three species. Density-functional theory (DFT) calculations show that these oxide clusters can be viewed as $B_4(BO)_n^-$ ($n = 1$–3), i.e., boronyl ligands coordinated to a rhombic B_4 cluster. The bare B_4 cluster is known to possess double (σ and π) aromaticity.[8,44] While the delocalized σ

a)Electronic mail: lisidian@sxu.edu.cn.
b)Electronic mail: lai-sheng_wang@brown.edu.

electrons are used to form localized σ bonds with the BO units, the π aromaticity remains intact in the three boron-boronyl clusters.

II. EXPERIMENTAL AND COMPUTATIONAL METHODS

A. Photoelectron spectroscopy

The experiment was carried out using a magnetic-bottle PES apparatus equipped with a laser vaporization cluster source, details of which were described in Refs. 45 and 46. Briefly, the $B_mO_n^-$ clusters were produced by laser vaporization of a pure disk target made of enriched ^{10}B isotope (99.75%) in the presence of a helium carrier gas seeded with 0.01% O_2 and analyzed using a time-of-flight mass spectrometer. The B_5O^-, $B_6O_2^-$, and $B_7O_3^-$ clusters of interest were each mass-selected and decelerated before being photodetached. Three detachment photon energies were used in the current experiment: 355 nm (3.496 eV) and 266 nm (4.661 eV) from a Nd:YAG laser and 193 nm (6.424 eV) from an ArF excimer laser. Photoelectrons were collected at nearly 100% efficiency by the magnetic bottle and analyzed in a 3.5 m long electron flight tube. The PES spectra were calibrated using the known spectra of Rh^- and Au^-, and the energy resolution of the apparatus was $\Delta E_k/E_k \approx 2.5\%$, that is, ~25 meV for 1 eV kinetic energy electrons.

B. Computational methods

The DFT structural searches were performed using the Coalescence-Kick (CK) global minimum search program developed by Boldyrev and co-workers,[12,47] initially at the hybrid B3LYP level[48] with the 3-21G basis set.[49] The top 15 low-lying candidate structures were then fully optimized at the same level with the augmented Dunning's all-electron basis set (aug-cc-pVTZ).[50] Frequency calculations were done to confirm that the obtained structures are true minima. Excitation energies of the neutral clusters were calculated with the time-dependent DFT (TDDFT) method[51] at the anion ground-state geometries. Single-point CCSD(T) (Ref. 52) calculations were done at the B3LYP/aug-cc-pVTZ geometries to further evaluate the relative energies of the top five low-lying structures, and to refine the ground-state adiabatic and vertical detachment energies (ADEs and VDEs). All calculations were done using the GAUSSIAN 03 package.[53]

III. EXPERIMENTAL RESULTS

A. B_5O^-

The PES spectra of B_5O^- are shown in Fig. 1 at three photon energies. The 355 nm spectrum (Fig. 1(a)) reveals a sharp band X, which defines an accurate ground state ADE and VDE of 3.45 ± 0.01 eV (Table I) and represents the electron affinity (EA) of the corresponding B_5O neutral. This sharp transition suggests that there is very little geometry change between the ground state of B_5O^- and its corresponding neutral state. At 266 nm (Fig. 1(b)), a very weak and short vibrational progression is resolved for band X. Two vibrational modes can be identified for the ground state of B_5O with frequencies of 1110 ± 50 and 1990 ± 50 cm^{-1}.

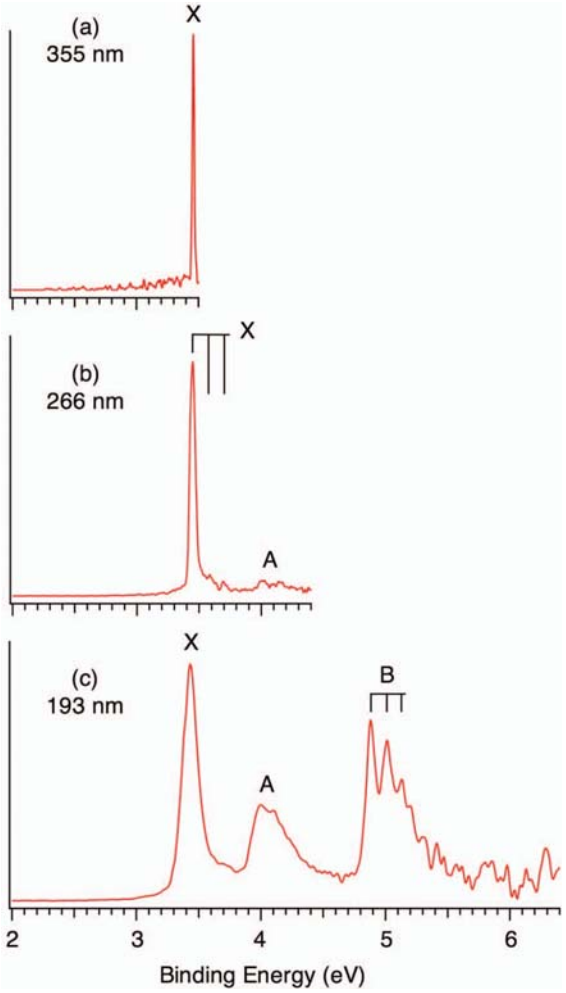

FIG. 1. Photoelectron spectra of B_5O^- at (a) 355 nm (3.496 eV), (b) 266 nm (4.661 eV), and (c) 193 nm (6.424 eV). The vertical lines represent vibrational structures.

The first excited state (band A) shows weak intensity at 266 nm with discernible fine structures and is significantly enhanced at 193 nm (Fig. 1(c)). A vibrational mode with a frequency of ~1130 cm^{-1} is estimated for this band, and a lower frequency mode (~700 cm^{-1}) is discernible. The VDE of band A is estimated from the peak center to be 4.05 eV. Band B (VDE: 4.88 eV) shows a partially resolved vibrational progression with a spacing of 1010 cm^{-1}. No prominent PES features are observed beyond ~5.5 eV.

B. $B_6O_2^-$

The 266 nm PES spectrum of $B_6O_2^-$ (Fig. 2(a)) shows a vibrational progression for band X, whose intense 0–0 transition at 3.54 ± 0.02 eV defines the ground state ADE and VDE and the EA of the corresponding neutral B_6O_2. Two vibrational modes are observed with frequencies of 980 ± 30 cm^{-1} and 2010 cm^{-1}. The first excited state band A is broad with unresolved vibrational structures at a VDE of

TABLE I. Experimental adiabatic (ADE) and vertical (VDE) detachment energies (in eV) and vibrational frequencies (in cm^{-1}) from the photoelectron spectra of B_5O^-, $B_6O_2^-$, and $B_7O_3^-$, as compared to those calculated from the global minimum structures (**1**, **3**, and **5**) at the B3LYP/aug-cc-pVTZ level of theory.

		Expt.			Theory (B3LYP)		
	Feature	ADE[a,b]	VDE[a]	Vib. freq.[a]	Final state	ADE[c]	VDE[c]
B_5O^-	X	3.45 (1)	3.45 (1)	1110 (50), 1990 (50)	$^2A_1$	3.17	3.20
	A		4.05 (5)	1130 (50)	$^2B_2$		4.14
	B		4.88 (3)	1010 (30), 2010 (30)	$^2B_1$		4.95
					$^2B_2$		6.12
$B_6O_2^-$	X	3.54 (2)	3.54 (2)	980 (30), ~2010	^1A_g	3.58	3.62
	A		4.53 (5)		$^3B_{3g}$		4.42
					$^1B_{3g}$		5.09
	B		5.20 (2)	~980	$^3B_{3u}$		5.11
					$^1B_{3u}$		5.69
$B_7O_3^-$	X	4.94 (5)	5.10 (5)		$^2B_2$	4.94	5.13
	A		5.78 (5)	~2000	$^2B_1$		5.90
	B		5.87 (5)	~2000	$^2A_1$		5.94
					$^2B_2$		7.61

[a]Numbers in the parentheses represent experimental uncertainties in the last digits.
[b]Electron affinity of the corresponding neutral cluster.
[c]The ground state ADE/VDE from the single-point CCSD(T)//B3LYP/aug-cc-pVTZ calculations are 3.43/3.48 eV for B_5O^-, 3.53/3.53 eV for $B_6O_2^-$, and 4.95/5.10 eV for $B_7O_3^-$.

4.53 eV (Fig. 2(b)). The second excited state band B shows a vibrational progression with an estimated frequency of ~980 cm^{-1}, and its 0–0 transition at 5.20 eV represents both the ADE and VDE for this transition.

C. $B_7O_3^-$

The electron binding energies for $B_7O_3^-$ are very high and its PES spectrum can only be measured at 193 nm, as shown in Fig. 3. Two broad bands are observed. The ground state band X shows unresolved vibrational structures. The ground state ADE is evaluated by drawing a straight line along the leading edge of band X and then adding the instrumental resolution to the intersection with the binding energy axis. The ADE thus determined is 4.94 ± 0.05 eV, which also represents the EA of the corresponding neutral B_7O_3. The ground state VDE is measured from the band maximum to be 5.10 eV. The higher binding energy band displays fine vibrational features. As will be shown below in the theoretical calculations, there are two closely lying detachment transitions contained in this band, which are identified tentatively as bands A and B with VDEs of 5.78 and 5.87 eV. Each band also exhibits a vibrational progression with similar spacings of ~2000 cm^{-1}.

The obtained ADE, VDEs, and vibrational frequencies are given in Table I for the three clusters and compared with calculated ADEs and VDEs.

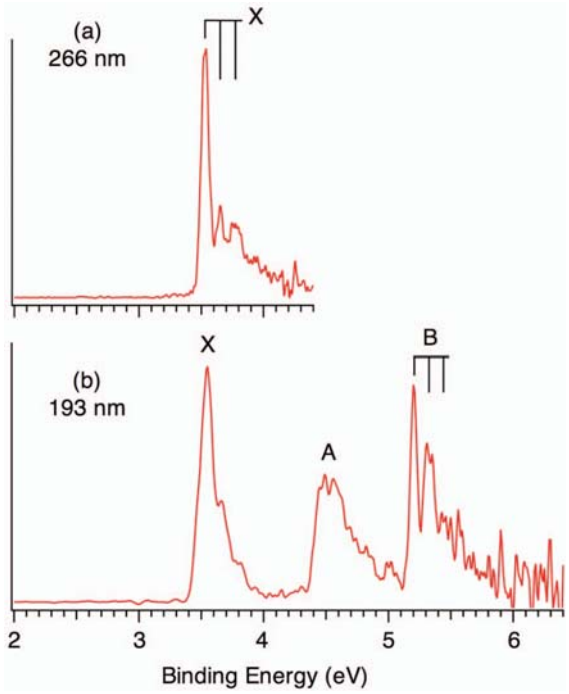

FIG. 2. Photoelectron spectra of $B_6O_2^-$ at (a) 266 nm and (b) 193 nm. The vertical lines represent vibrational structures.

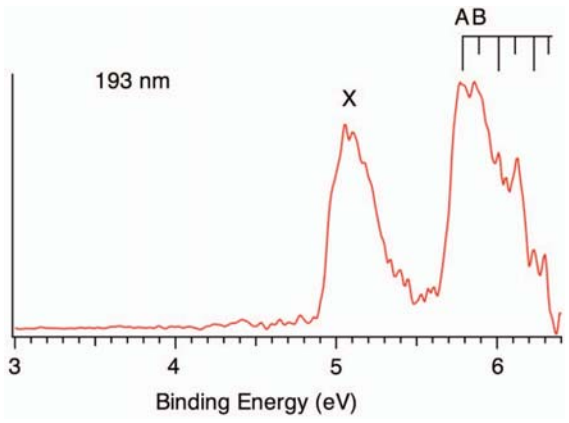

FIG. 3. Photoelectron spectrum of $B_7O_3^-$ at 193 nm. The vertical lines represent vibrational structures.

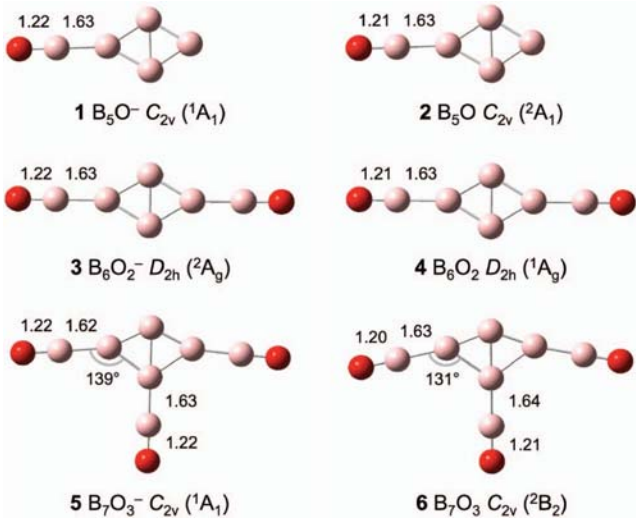

FIG. 4. Optimized global minimum anion structures (**1**, **3**, and **5**) for the B_5O^-, $B_6O_2^-$, and $B_7O_3^-$ clusters at the B3LYP/aug-cc-pVTZ level, along with their corresponding neutral structures (**2**, **4**, and **6**). The B≡O triple and B−(B≡O) single bond lengths are given in Å.

IV. THEORETICAL RESULTS

A. Optimized cluster structures

Structural searches were performed initially using the CK method[12,47] and then fully optimized at the B3LYP/aug-cc-pVTZ level. The top 15 low-lying candidate structures for each cluster are summarized in Figs. S1–S3 along with their relative energies, as supplementary materials.[54] The energies of the top 5 structures were further evaluated at the single-point CCSD(T) level. For the anionic clusters, the global minimum of each species can be viewed as one, two, and three BO units coordinated to a rhombic B_4 core for B_5O^-, $B_6O_2^-$, and $B_7O_3^-$, respectively. These structures are given in Fig. 4 (**1**, **3**, **5**) with key structural parameters. The next low-lying isomer is more than 29 kcal/mol higher in energy for B_5O^- and $B_7O_3^-$, and more than 13 kcal/mol higher for $B_6O_2^-$ at the single point CCSD(T) level (Figs. S1–S3).[54] These results suggest that there could be no low-lying isomers populated in the cluster beam for any of the anionic clusters.

However, the global minima for neutral B_5O and B_6O_2 are different from that of the anion. In the global minimum of B_5O, the O atom bridges two B atoms on the peripheral of the planar B_5 cluster. The corresponding isomer that is similar to the global minimum of the anion is 3.6 kcal/mol higher in energy at the single point CCSD(T) level [Fig. S1(b)].[54] The global minimum of B_6O_2 involves one BO unit coordinated to the global minimum of B_5O [Fig. S2(b)].[54] The global minimum of B_7O_3 is similar to that of its anion [Fig. S3(b)],[54] although the isomer with two BO units coordinated to the global minimum of B_5O is almost degenerate at the single point CCSD(T) level. The structures of B_5O^-, B_5O, $B_6O_2^-$, and B_6O_2 have been calculated previously.[33,34] The current results are consistent with those reported in Refs. 33 and 34. It should be pointed out that in cases, where the neutrals and the anions have different global minima, the spectroscopic information obtained from the PES data concerns about the neutral isomers that have structures closest to the anionic global minima, because photodetachment is a vertical transition, governed by the Franck-Condon principle.

TABLE II. Calculated top apex ∠BBB bond angles and its changes in the rhombic B_4 core from the anion to neutral, at the B3LYP level, for $B_4(BO)_n^-$ and $B_4(BO)_n$ ($n = 1$–3) (see Fig. 4).

	Bond angle	Neutral	Bond angle	Angle change
B_5O^- (**1**)	117°	B_5O (**2**)	115°	−2°
$B_6O_2^-$ (**3**)	116°	B_6O_2 (**4**)	118°	+2°
$B_7O_3^-$ (**5**)	126°	B_7O_3 (**6**)	138°	+12°

B. Geometrical changes from the anions to neutrals

The neutral cluster structures relevant to the PES experiment are compared with the corresponding anionic global minima in Fig. 4 (**2**, **4**, and **6**). The symmetries of all three neutral clusters are the same as that of the anionic global minima. Geometric changes are very small between the neutral structures of B_5O (**2**) and B_6O_2 (**4**) and their respective anions, consistent with the sharp ground state PES band in each case (Figs. 1 and 2). The BO bond lengths are shortened from 1.22 to 1.21 Å upon electron detachment in each case, suggesting that the BO stretching mode should be active in the ground state detachment band. In addition, there is a slight elongation of the shorter diagonal B–B distance in the rhombic B_4 core in B_5O^- (**1**) by 0.04 Å upon electron detachment, resulting in a slight reduction of the top ∠BBB apex angle from 117° in **1** to 115° in **2**, as given in Table II. This geometry change suggests that a vibrational mode involving the breathing of the B_4 core should also be active during photodetachment. In the case of $B_6O_2^-$, there is a slight shortening of the shorter diagonal B–B bond length upon electron detachment, resulting in a slight increase of the top ∠BBB apex angle in the rhombic B_4 unit from 116° in **3** to 118° in **4** (Table II). Again, a vibrational mode involving the B_4 framework is expected to be active in the ground state detachment band of $B_6O_2^-$. The geometrical changes of $B_7O_3^-$ (**5**) upon electron detachment are more significant, including a shortening of the shorter diagonal B–B distance in the B_4 core by 0.07 Å, that results in a substantial expansion of the top ∠BBB apex bond angle by 12° (Table II). Furthermore, the bond angles of two of the boronyl units become more bent by 8° relative to the B_4 core in the neutral, as shown in Fig. 4. All these geometry changes suggest that many vibrational modes would be active upon electron detachment from $B_7O_3^-$, giving rise to broad PES features, in agreement with experimental observations (Fig. 3).

V. COMPARISON BETWEEN EXPERIMENT AND THEORY

A. B_5O^-

The global minimum of B_5O^- (**1**, C_{2v}, $^1A_1$) has a closed-shell electron configuration of $\ldots b_1^2 b_2^2 a_1^2$. Plots of the occupied valence molecular orbitals (MOs) are shown in Fig. S4 in

the supplementary material.[54] Electron detachment from the highest occupied MO (HOMO, a_1) reaches the neutral state **2** (C_{2v}, $^2A_1$). As shown in Table I, the calculated ADE (3.17 eV) and VDE (3.20 eV) at the B3LYP/aug-cc-pVTZ level for this detachment channel are lower than the experimental values (3.45 eV) by about 0.2−0.3 eV. However, our single-point CCSD(T)//B3LYP/aug-cc-pVTZ data (ADE: 3.43 eV; VDE: 3.48 eV) are in excellent agreement with the experimental values. The two observed vibrational modes should correspond to the B–O stretching (1990 cm^{-1}) in the boronyl unit and the B–B stretching (1110 cm^{-1}) in the B_4 core. These observed frequencies are also in good agreement with the calculated values (Table S1). The first two excited states are due to electron detachment from the HOMO−1 (b_2) and HOMO−2 (b_1), respectively. The calculated VDEs at TDDFT level for these two detachment channels are 4.14 and 4.95 eV, in good agreement with the experimental values for band A (VDE: 4.05 eV) and band B (VDE: 4.88 eV), respectively.

B. $B_6O_2^-$

The global minimum of $B_6O_2^-$ (**3**, D_{2h}, ^2A_g) has an electron configuration of $\ldots b_{3u}^2 b_{3g}^2 a_g^1$. Plots of the valence MOs are shown in Fig. S5 in the supplementary material.[54] Electron detachment from the a_g HOMO results in the neutral state **4** (D_{2h}, ^1A_g) with a calculated ADE of 3.58 eV and VDE of 3.62 eV at the B3LYP/aug-cc-pVTZ level, in good agreement with the observed values for band X (3.54 eV). Again, the single-point CCSD(T)//B3LYP/aug-cc-pVTZ values (ADE: 3.53 eV; VDE: 3.53 eV) are almost in exact agreement with the experiment. The two observed vibrational modes (2010 and 980 cm^{-1}) should also correspond to the B–O stretching of the boronyl unit and the B–B stretching involving the B_4 core. These observations are also in good agreement with the calculated values (Table S1).

Because $B_6O_2^-$ has one unpaired electron, detachment of an electron of β or α spin from HOMO−1 (b_{3g}), would produce a triplet ($^3B_{3g}$) or singlet ($^1B_{3g}$) final states. The calculated VDEs for the $^3B_{3g}$ and $^1B_{3g}$ final states at TDDFT level are 4.42 and 5.09 eV, respectively. The calculated VDE for the $^3B_{3g}$ state is in good agreement with the observed VDE of band A (4.53 eV). The detachment channel leading to the singlet state should have lower relative intensity. In fact, the weak peak observed at ∼5.0 eV in the 193 nm spectrum (Fig. 2(b)) should correspond to the $^1B_{3g}$ state. Similarly, electron detachment from HOMO−2 (b_{3u}) is predicted to result in two final states $^3B_{3u}$ (5.11 eV) and $^1B_{3u}$ (5.69 eV), where the triplet state is again in good agreement with band B (VDE: 5.20 eV) and the singlet state may be buried in the higher binding energy part of band B in the 193 nm spectrum (Fig. 2(b)).

C. $B_7O_3^-$

The global minimum of $B_7O_3^-$ (**5**, C_{2v}, $^1A_1$) possesses a closed-shell configuration of $\ldots b_1^2 a_1^2 b_2^2$. Plots of its occupied valence MOs are given in Fig. S6.[54] Photodetachment from the b_2 HOMO reaches the neutral ground state **6** (C_{2v}, $^2B_2$). The predicted ADE/VDE, 4.94/5.13 and 4.95/5.10 eV at the B3LYP and CCSD(T) levels, respectively, are both in excellent agreement with the experimental values for band X (ADE: 4.94 eV; VDE: 5.10 eV), as shown in Table I. The broad band X is consistent with the large geometry changes between the ground state of $B_7O_3^-$ (**5**) and its corresponding neutral (**6**). The next two detachment channels from HOMO-1 and HOMO-2 give very close VDEs: 5.90 eV from the b_1 orbital and 5.94 eV from the a_1 orbital. These calculated values are also consistent with the observed broad band at ∼6 eV.

The excellent overall agreement between the theoretical calculations and experimental observations for B_5O^-, $B_6O_2^-$, and $B_7O_3^-$ lends considerable credence to the global minima identified for these oxide clusters.

VI. DISCUSSION

A. Isolobal analogy between boron-rich $B_mO_n^-$ clusters and boranes

The global minimum structures of B_5O^- (**1**), $B_6O_2^-$ (**3**), and $B_7O_3^-$ (**5**) can be formulated as $B_4(BO)_n^-$ ($n = 1$–3), i.e., as boronyl ligands coordinated to a rhombic B_4 unit. These clusters are in line with our prior findings that all boron-rich oxide clusters, $B_mO_n^-$, can be formulated as boronyls coordinated to a boron core, $B_{m-n}(BO)_n^-$.[39–43] Chemically, the boronyl groups act as σ radicals, akin to the H atom. Indeed, valent isoelectronic boron hydride clusters, such as B_4H_n ($n = 1$–3) and $B_4H_3^-$, have been computed,[55] which have similar ground-state structures as the corresponding $B_4(BO)_n$ or $B_4(BO)_3^-$ clusters. The current results further extend the isolobal analogy between boron-rich boron oxide clusters and boranes. We further note that the bare B_4^- cluster is rather floppy,[8] while the B_4 framework in the $B_4(BO)_n^-$ clusters is much more rigid as a result of BO binding.

B. Chemical bonding in $B_4(BO)_n^-$ ($n = 1$–3) and π aromaticity

The chemical bonding in the boron-boronyl clusters can be elucidated using the adaptive natural density partitioning (AdNDP) method.[44] AdNDP represents the electronic structure of a molecule in terms of n-center two-electron (nc-2e) bonds, with the n value ranging from one to the total number of atoms in the molecule. AdNDP recovers the classical Lewis bonding elements (lone pairs and 2c-2e bonds), as well as nonclassical delocalized nc-2e bonds. Since the current version of the AdNDP program only deals with closed-shell systems,[44] we analyzed the bonding of B_5O^- (**1**, $^1A_1$), B_6O_2 (**4**, ^1A_g), and $B_7O_3^-$ (**5**, $^1A_1$), as shown in Fig. 5. The AdNDP analyses of B_4 (D_{2h}, ^1A_g) and B_4^{2-} (D_{2h}, ^1A_g) are included for comparison.[8,44]

The bare B_4 cluster consists of four 2c-2e B–B bonds, one delocalized σ and one delocalized π bond, making it doubly aromatic, whereas B_4^{2-} has two delocalized σ bonds and one delocalized π bond, making it σ antiaromatic and π aromatic.[8,44] The AdNDP analyses for the boron-boronyl clusters readily recover the 2c-2e B≡O triple bonds, 2c-2e B−(B≡O) single bonds, and O 2s lone pairs, as shown in

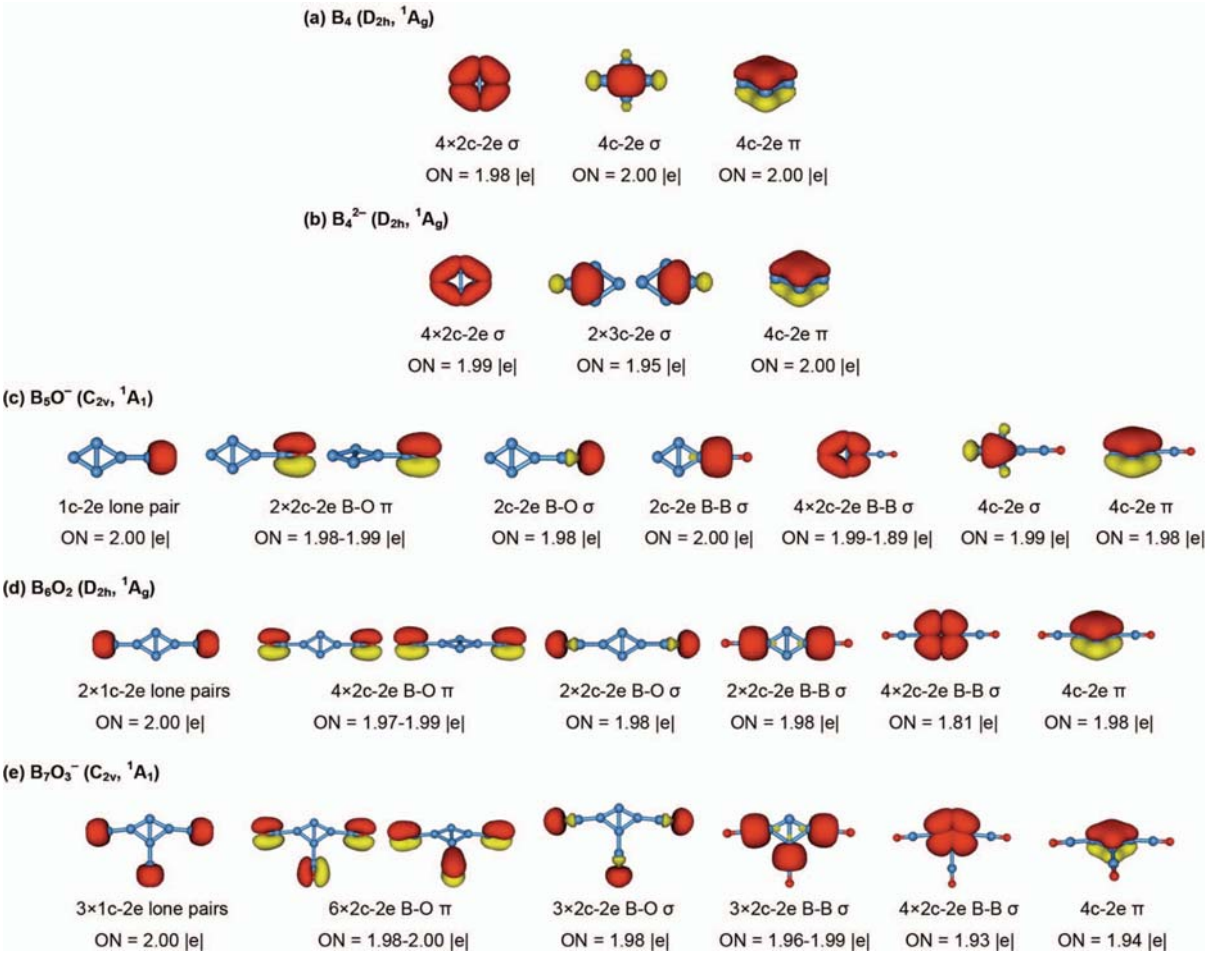

FIG. 5. Adaptive natural density partitioning (AdNDP) analyses for the closed-shell B_5O^- (**1**, $^1A_1$), B_6O_2 (**4**, ^1A_g), and $B_7O_3^-$ (**5**, $^1A_1$) in comparison with that of B_4 (D_{2h}, ^1A_g), and B_4^{2-} (D_{2h}, ^1A_g). The occupation numbers (ONs) are indicated.

Fig. 5. The former are localized bonding elements within the boronyl groups and in between the B_4 core and the boronyl groups. The triple B≡O bond and the single B−(B≡O) bond distances are typical, centering at 1.22 and 1.62–1.63 Å in $B_4(BO)_n^-$, in comparison to those calculated for the B≡O triple bond in BO^- (1.234 Å) and the single B−(B≡O) bond in $B_2(BO)_2^-$ (1.607 Å) at the same level of theory.[26,40] The delocalized σ electrons in B_4 are used to form B–BO bonds, whereas the delocalized π bond is intact in all the $B_4(BO)_n^-$ clusters, which can still be viewed as π aromatic.

VII. CONCLUSIONS

We have investigated the electronic and structural properties of a series of boron oxide clusters, B_5O^-, $B_6O_2^-$, and $B_7O_3^-$ using photoelectron spectroscopy and theoretical calculations. Vibrationally resolved photoelectron spectra are obtained. Density-functional calculations show that global minima of these oxide clusters can be formally formulated as $B_4(BO)_n^-$ (n = 1–3), which involve the coordination of boronyl ligands to a rhombic B_4 core. Chemical bonding analyses indicate that the delocalized σ electrons in the B_4 core are used to form σ bonds with the boronyl ligands, whereas π aromaticity in the B_4 core remains intact upon boron boronyl coordination in the series of clusters. The current study shows further that the boronyl ligand plays an important role as structural features in boron-rich boron oxide clusters.

ACKNOWLEDGMENTS

This work was supported by the US National Science Foundation (NSF) (DMR-0904034 to L.-S.W.) and the National Natural Science Foundation of China (NNSFC) (No. 20873117 to S.-D.L.).

[1]N. N. Greenwood and A. Earnshaw, *Chemistry of the Elements*, 2nd ed. (Butterworth-Heinemann, Oxford, 1997).
[2]F. A. Cotton, G. Wilkinson, C. A. Murrillo, and M. Bochmann, *Advanced Inorganic Chemistry*, 6th ed. (Wiley, New York, 1999).
[3]W. N. Lipscomb, *Boron Hydrides* (Benjamin, New York, 1963).
[4]W. N. Lipscomb, Science **196**, 1047 (1977).
[5]L. Hanley, J. L. Whitten, and S. L. Anderson, J. Phys. Chem. **92**, 5803 (1988); P. A. Hintz, S. A. Ruatta, and S. L. Anderson, J. Chem. Phys. **92**, 292 (1990); S. A. Ruatta, P. A. Hintz, and S. L. Anderson, *ibid.* **94**, 2833 (1991); M. B. Sowa-Resat, J. Smolanoff, A. Lapiki, and S. L. Anderson, *ibid.* **106**, 9511 (1997).
[6]H. Kato, K. Yamashita, and K. Morokuma, Chem. Phys. Lett. **190**, 361 (1992); R. Kawai and J. H. Weare, *ibid.* **191**, 311 (1992); J. M. L. Martin, J. P. Francois, and R. Gijbels, *ibid.* **189**, 529 (1992); A. Ricca and C. W. Bauschlicher, Jr., Chem. Phys. **208**, 233 (1996); J. Niu, B. K. Rao, and P. Jena, J. Chem. Phys. **107**, 132 (1997); F. L. Gu, X. M. Yang, A. C. Tang,

H. J. Jiao, and P. v. R. Schleyer, J. Comput. Chem. **19**, 203 (1998); J. O. C. Jiménez-Halla, R. Islas, T. Heine, and G. Merino, Angew. Chem. Int. Ed. **49**, 5668 (2010).
[7]I. Boustani, Int. J. Quant. Chem. **52**, 1081 (1994); Phys. Rev. B **55**, 16426 (1997).
[8]H. J. Zhai, L. S. Wang, A. N. Alexandrova, A. I. Boldyrev, and V. G. Zakrzewski, J. Phys. Chem. A **107**, 9319 (2003).
[9]H. J. Zhai, L. S. Wang, A. N. Alexandrova, and A. I. Boldyrev, J. Chem. Phys. **117**, 7917 (2002).
[10]A. N. Alexandrova, A. I. Boldyrev, H. J. Zhai, L. S. Wang, E. Steiner, and P. W. Fowler, J. Phys. Chem. A **107**, 1359 (2003).
[11]A. N. Alexandrova, A. I. Boldyrev, H. J. Zhai, and L. S. Wang, J. Phys. Chem. A **108**, 3509 (2004).
[12]A. P. Sergeeva, B. B. Averkiev, H. J. Zhai, A. I. Boldyrev, and L. S. Wang, J. Chem. Phys. **134**, 224304 (2011).
[13]H. J. Zhai, A. N. Alexandrova, K. A. Birch, A. I. Boldyrev, and L. S. Wang, Angew. Chem. Int. Ed. **42**, 6004 (2003); H. J. Zhai, B. Kiran, J. Li, and L. S. Wang, Nature Mater. **2**, 827 (2003); A. P. Sergeeva, D. Yu. Zubarev, H. J. Zhai, A. I. Boldyrev, and L. S. Wang, J. Am. Chem. Soc. **130**, 7244 (2008); W. Huang, A. P. Sergeeva, H. J. Zhai, B. B. Averkiev, L. S. Wang, and A. I. Boldyrev, Nature Chem. **2**, 202 (2010).
[14]B. Kiran, S. Bulusu, H. J. Zhai, S. Yoo, X. C. Zeng, and L. S. Wang, Proc. Natl. Acad. Sci. U.S.A. **102**, 961 (2005).
[15]A. N. Alexandrova, H. J. Zhai, L. S. Wang, and A. I. Boldyrev, Inorg. Chem. **43**, 3552 (2004); A. N. Alexandrova, A. I. Boldyrev, H. J. Zhai, and L. S. Wang, J. Chem. Phys. **122**, 054313 (2005); H. J. Zhai, L. S. Wang, D. Yu. Zubarev, and A. I. Boldyrev, J. Phys. Chem. A **110**, 1689 (2006); L. M. Wang, W. Huang, B. B. Averkiev, A. I. Boldyrev, and L. S. Wang, Angew. Chem. Int. Ed. **46**, 4550 (2007); B. B. Averkiev, D. Yu. Zubarev, L. M. Wang, W. Huang, L. S. Wang, and A. I. Boldyrev, J. Am. Chem. Soc. **130**, 9248 (2008); B. B. Averkiev, L. M. Wang, W. Huang, L. S. Wang, and A. I. Boldyrev, Phys. Chem. Chem. Phys. **11**, 9840 (2009); C. Romanescu, A. P. Sergeeva, W. L. Li, A. I. Boldyrev, and L. S. Wang, J. Am. Chem. Soc. **133**, 8646 (2011); T. R. Galeev, C. Romanescu, W. L. Li, L. S. Wang, and A. I. Boldyrev, J. Chem. Phys. **135**, 104301 (2011); W. L. Li, C. Romanescu, T. R. Galeev, L. S. Wang, and A. I. Boldyrev, J. Phys. Chem. A **115**, 10391 (2011); C. Romanescu, T. R. Galeev, W. L. Li, A. I. Boldyrev, and L. S. Wang, Angew. Chem. Int. Ed. **50**, 9334 (2011); T. R. Galeev, C. Romanescu, W. L. Li, L. S. Wang, and A. I. Boldyrev, *ibid.* **51**, 2101 (2012); W. L. Li, C. Romanescu, T. R. Galeev, Z. Piazza, A. I. Boldyrev, and L. S. Wang, J. Am. Chem. Soc. **134**, 165 (2012).
[16]A. N. Alexandrova, A. I. Boldyrev, H. J. Zhai, and L. S. Wang, Coord. Chem. Rev. **250**, 2811 (2006); D. Yu. Zubarev and A. I. Boldyrev, J. Comput. Chem. **28**, 251 (2007).
[17]Z. A. Piazza, W. L. Li, C. Romanescu, A. P. Sergeeva, L. S. Wang, and A. I. Boldyrev, J. Chem. Phys. **136**, 104310 (2012).
[18]T. B. Tai, N. M. Tam, and M. T. Nguyen, Chem. Phys. Lett. **530**, 71 (2012).
[19]F. Li, P. Jin, D. Jiang, L. Wang, S. B. Zhang, J. Zhao, and Z. Chen, J. Chem. Phys. **136**, 074302 (2012).
[20]E. Oger, N. R. M. Crawford, R. Kelting, P. Weis, M. M. Kappes, and R. Ahlrichs, Angew. Chem. Int. Ed. **46**, 8503 (2007).
[21]J. E. Fowler and J. M. Ugalde, J. Phys. Chem. A **104**, 397 (2000); J. I. Aihara, *ibid.* **105**, 5486 (2001); J. I. Aihara, H. Kanno, and T. Ishida, J. Am. Chem. Soc. **127**, 13324 (2005).
[22]H. Tang and S. Ismail-Beigi, Phys. Rev. Lett. **99**, 115501 (2007).
[23]T. R. Galeev, Q. Chen, J. C. Guo, H. Bai, C. Q. Miao, H. G. Lu, A. P. Sergeeva, S. D. Li, and A. I. Boldyrev, Phys. Chem. Chem. Phys. **13**, 11575 (2011).
[24]S. H. Bauer, Chem. Rev. **96**, 1907 (1996).
[25]P. G. Wenthold, J. B. Kim, K. L. Jonas, and W. C. Lineberger, J. Phys. Chem. A **101**, 4472 (1997).
[26]H. J. Zhai, L. M. Wang, S. D. Li, and L. S. Wang, J. Phys. Chem. A **111**, 1030 (2007).
[27]E. R. Lory and R. F. Porter, J. Am. Chem. Soc. **93**, 6301 (1971); B. M. Ruscic, L. A. Curtiss, and J. Berkowitz, J. Chem. Phys. **80**, 3962 (1984); Y. Kawashima, Y. Endo, K. Kawaguchi, and E. Hirota, Chem. Phys. Lett. **135**, 441 (1987); H. Bock, L. Cederbaum, W. von Niessen, P. Paetzold, P. Rosmus, and B. Solouki, Angew. Chem. Int. Ed. Engl. **28**, 88 (1989).
[28]W. Weltner, Jr. and J. R. W. Warn, J. Chem. Phys. **37**, 292 (1962); A. Sommer, D. White, M. J. Linevsky, and D. E. Mann, *ibid.* **38**, 87 (1963); R. J. Doyle, Jr., J. Am. Chem. Soc. **110**, 4120 (1988).
[29]L. Hanley and S. L. Anderson, J. Chem. Phys. **89**, 2848 (1988); D. Peiris, A. Lapicki, S. L. Anderson, R. Napora, D. Linder, and M. Page, J. Phys. Chem. A **101**, 9935 (1997).
[30]T. R. Burkholder and L. Andrews, J. Chem. Phys. **95**, 8697 (1991); D. V. Lanzisera and L. Andrews, J. Phys. Chem. A **101**, 1482 (1997).
[31]A. M. McAnoy, S. Dua, D. Schroder, J. H. Bowie, and H. Schwarz, J. Phys. Chem. A **107**, 1181 (2003); A. M. McAnoy, S. Dua, D. Schroder, J. H. Bowie, and H. Schwarz, *ibid.* **108**, 2426 (2004).
[32]M. Zhou, L. Jiang, and Q. Xu, Chem. Eur. J. **10**, 5817 (2004).
[33]T. B. Tai, M. T. Nguyen, and D. A. Dixon, J. Phys. Chem. A **114**, 2893 (2010).
[34]C. B. Shao, L. Jin, and Y. H. Ding, J. Comput. Chem. **32**, 771 (2011).
[35]A. V. Nemukhin and F. Weinhold, J. Chem. Phys. **98**, 1329 (1993); M. L. Drummond, V. Meunier, and B. G. Sumpter, J. Phys. Chem. A **111**, 6539 (2007); X. J. Feng, Y. H. Luo, X. Liang, L. X. Zhao, and T. T. Cao, J. Cluster Sci. **19**, 421 (2008); T. B. Tai and M. T. Nguyen, Chem. Phys. Lett. **483**, 35 (2009); M. T. Nguyen, M. H. Matus, V. T. Ngan, D. J. Grant, and D. A. Dixon, J. Phys. Chem. A **113**, 4895 (2009); C. B. Shao, L. Jin, L. J. Fu, and Y. H. Ding, Mol. Phys. **107**, 2395 (2009); Theor. Chem. Acc. **124**, 161 (2009).
[36]S. D. Li, C. Q. Miao, J. C. Guo, and G. M. Ren, J. Comput. Chem. **26**, 799 (2005); G. M. Ren, S. D. Li, and C. Q. Miao, THEOCHEM **770**, 193 (2006).
[37]H. Braunschweig, K. Radacki, and A. Schneider, Science **328**, 345 (2010).
[38]D. Yu. Zubarev, A. I. Boldyrev, J. Li, H. J. Zhai, and L. S. Wang, J. Phys. Chem. A **111**, 1648 (2007).
[39]H. J. Zhai, S. D. Li, and L. S. Wang, J. Am. Chem. Soc. **129**, 9254 (2007).
[40]S. D. Li, H. J. Zhai, and L. S. Wang, J. Am. Chem. Soc. **130**, 2573 (2008).
[41]W. Z. Yao, J. C. Guo, H. G. Lu, and S. D. Li, J. Phys. Chem. A **113**, 2561 (2009).
[42]H. J. Zhai, C. Q. Miao, S. D. Li, and L. S. Wang, J. Phys. Chem. A **114**, 12155 (2010).
[43]H. J. Zhai, J. C. Guo, S. D. Li, and L. S. Wang, Chem. Phys. Chem. **12**, 2549 (2011).
[44]D. Yu. Zubarev and A. I. Boldyrev, Phys. Chem. Chem. Phys. **10**, 5207 (2008).
[45]L. S. Wang, H. S. Cheng, and J. Fan, J. Chem. Phys. **102**, 9480 (1995).
[46]L. S. Wang and H. Wu, in *Advances in Metal and Semiconductor Clusters*, Cluster Materials Vol. 4, edited by M. A. Duncan (JAI, Greenwich, CT, 1998), pp. 299–343.
[47]M. Saunders, J. Comput. Chem. **25**, 621 (2004); P. P. Bera, K. W. Sattelmeyer, M. Saunders, and P. v. R. Schleyer, J. Phys. Chem. A **110**, 4287 (2006).
[48]A. D. Becke, J. Chem. Phys. **98**, 5648 (1993); C. Lee, W. Yang, and R. G. Parr, Phys. Rev. B **37**, 785 (1988).
[49]J. S. Binkley, J. A. Pople, and W. J. Hehre, J. Am. Chem. Soc. **102**, 939 (1980).
[50]R. A. Kendall, T. H. Dunning, and R. J. Harrison, J. Chem. Phys. **96**, 6796 (1992).
[51]M. E. Casida, C. Jamorski, K. C. Casida, and D. R. Salahub, J. Chem. Phys. **108**, 4439 (1998); R. Bauernschmitt and R. Ahlrichs, Chem. Phys. Lett. **256**, 454 (1996).
[52]J. Cizek, Adv. Chem. Phys. **14**, 35 (1969); G. E. Scuseria and H. F. Schaefer, J. Chem. Phys. **90**, 3700 (1989); R. J. Bartlett and M. Musial, Rev. Mod. Phys. **79**, 291 (2007).
[53]M. J. Frisch, G. W. Trucks, H. B. Schlegel *et al.*, GAUSSIAN 03, revision A.1, Gaussian, Inc., Pittsburgh, PA, 2003.
[54]See supplementary material at http://dx.doi.org/10.1063/1.4737863 for the calculated structures of B_5O^-, $B_6O_2^-$, $B_7O_3^-$, and their neutrals, as well as the occupied valence molecular orbitals for the global minima of B_5O^-, $B_6O_2^-$, $B_7O_3^-$.
[55]M. Böyökata, C. Ozdogan, and Z. B. Guvenc, THEOCHEM **805**, 91 (2007); M. L. McKee, Inorg. Chem. **38**, 321 (1999).